Personalized treatment for von Willebrand disease by RNA-targeted therapies

Jong, A. de

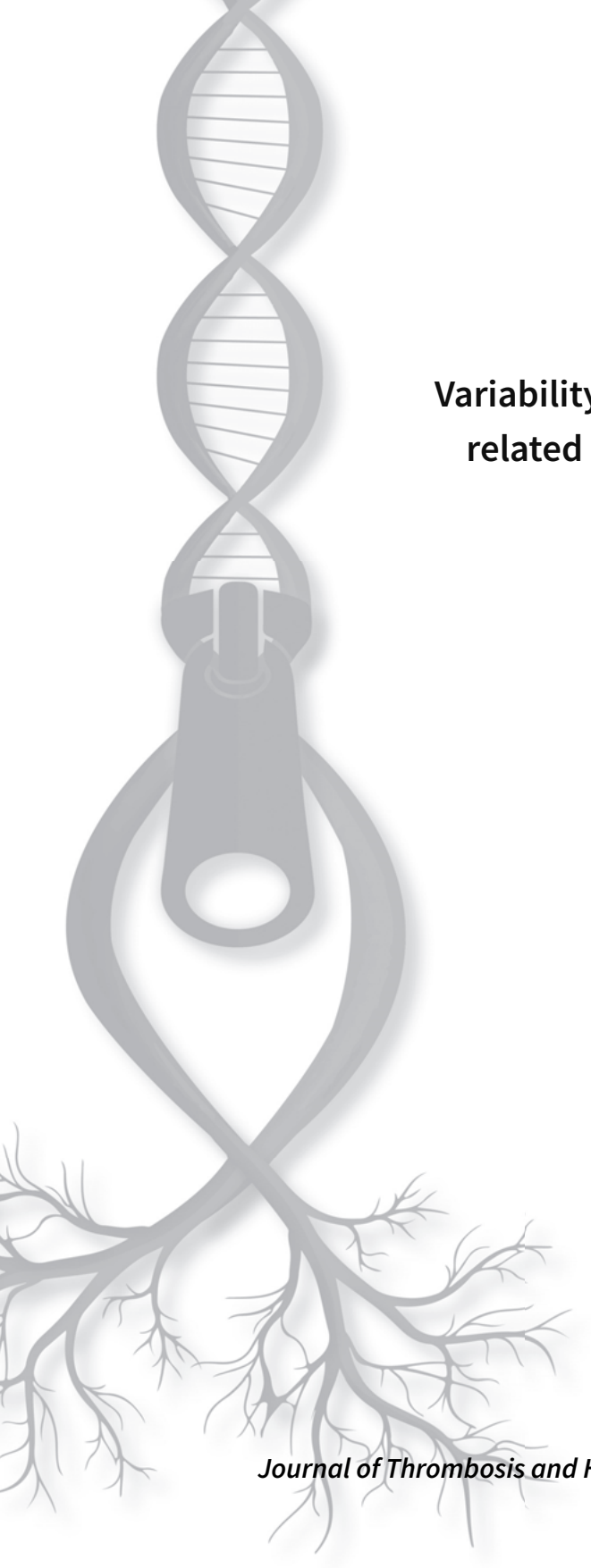

5

Variability of von Willebrand factor-related parameters in endothelial colony forming cells

Annika de Jong
Ester Weijers
Richard Dirven
Suzan de Boer
Jasmin Streur
Jeroen Eikenboom

Journal of Thrombosis and Haemostasis (2019) 17(9):1544-1554

Abstract

Background Endothelial colony forming cells (ECFCs) are cultured endothelial cells derived from peripheral blood. ECFCs are a powerful tool to study pathophysiological mechanisms underlying vascular diseases, including von Willebrand disease. In prior research, however, large variations between ECFC lines were observed in, among others, von Willebrand factor (VWF) expression. ***Objective*** Understand the relation between phenotypic characteristics and VWF-related parameters of healthy control ECFCs. ***Methods*** ECFC lines (N = 16) derived from six donors were studied at maximum cell density. Secreted and intracellular VWF antigen were measured by ELISA. The angiogenic capacity of ECFCs was investigated by the Matrigel tube formation assay. Differences in expression of genes involved in angiogenesis, aging, and endothelial to mesenchymal transition (EndoMT) were measured by quantitative PCR. ***Results*** Different ECFC lines show variable morphologies and cell density at maximum confluency and cell lines with a low maximum cell density show a mixed and more mesenchymal phenotype. We identified a significant positive correlation between maximum cell density and VWF production, both at protein and mRNA level. Also, significant correlations were observed between maximum cell density and several angiogenic, aging and EndoMT parameters. ***Conclusions*** We observed variations in morphology, maximum cell density, VWF production, and angiogenic potential between healthy control ECFCs. These variations seem to be attributable to differences in aging and EndoMT. Because variations correlate with cell density, we believe that ECFCs maintain a powerful tool to study vascular diseases. It is however important to compare cell lines with the same characteristics and perform experiments at maximum cell density.

Introduction

von Willebrand factor (VWF) is a large multimeric glycoprotein required for hemostasis. Generally, VWF is known as carrier protein for coagulation factor VIII and as mediator for platelet adhesion and aggregation at sites of vascular damage. More recently, other functions of VWF on the cellular level are described, for example in the process of angiogenesis.[1] Dysfunction or deficiencies of VWF lead to von Willebrand disease (VWD), the most common inherited bleeding disorder.[2] VWF is mainly synthesized in endothelial cells and stored in Weibel-Palade bodies.[3] A small proportion of VWF is produced in megakaryocytes, and stored in their alpha-granules.[4] The pathophysiology of VWD has historically been studied on a cellular level in heterologous cell systems by overexpression of VWF variants.[5,6] Yet, several aspects of VWF biology (i.e., the process of angiogenesis and VWF behavior under flow) can only be studied in endothelial cells. Moreover, because endothelial cells are the main source of VWF production, it is of utmost importance to study these cells in great detail to understand cellular defects in VWF to benefit VWD patients.

Obtaining endothelial cells from patients or healthy subjects used to be difficult because of the type of tissue needed for endothelial cell isolations. The source of endothelial cells mostly used is the umbilical vein, yielding human umbilical vein endothelial cells (HUVECs). However, the experimental use of HUVECs is limited because they cannot be obtained from subjects with specific clinical or genetic characteristics. Nowadays, endothelial cells can be isolated from the mononuclear cell fraction from peripheral blood and have the ability to expand *ex vivo*.[7,8] Cultured endothelial cells derived from peripheral blood have adopted different names in literature, such as blood outgrowth endothelial cells, late outgrowth endothelial cells or endothelial colony forming cells (ECFCs).[9] Recently, consensus was made to use the term ECFC and we will therefore adapt to this consensus. We would like to highlight that the ECFCs in this study are the same type of cells as the cells denoted as blood outgrowth endothelial cells used in prior studies published by us and most groups studying VWD pathophysiology.[10-12] In the past decade, multiple studies showed interesting results applying ECFCs to study VWD pathophysiology at the cellular level.[10-15] Unfortunately, these studies also showed a wide range of variation in the endothelial cells from VWD patients complicating interpretation and comparison of the results.[16] To confidently use ECFCs to study VWD pathophysiology, we need to understand the extent of these variations and their effects on VWF-related parameters; therefore we aim to understand the relation between the phenotypic characteristics and VWF-related parameters of ECFCs from healthy controls. We cultured ECFC lines and investigated their phenotypic characteristics in a standardized setup. The phenotypic characteristics of individual ECFC lines were correlated with VWF parameters and their angiogenic capacity. In addition, gene expression of specific pathways was investigated to unravel the potential underlying mechanism of ECFC variability.

Materials and methods

ECFC isolation

ECFCs were isolated according to Martin-Ramirez *et al* (2012).[17] In short, 30-80 mL peripheral blood was drawn in 10 mL trisodium citrate tubes (ECFCs 1 and 2; S-Monovette®#02.1067.001, Sarstedt, Nümbrecht, Germany) or 10 mL lithium heparin tubes (ECFCs 3-6; BD Biosciences Vacutainer #367880, BD, Erebodegem, Belgium). Peripheral blood was diluted 1:1 with phosphate-buffered saline (PBS) and blood components were separated by gradient centrifugation over Ficoll Paque (LUMC Pharmacy, Leiden, the Netherlands). The mononuclear cell fraction was isolated and washed 1x in PBS and 1x in 5 mL EGM-20 culture medium, consisting of 500 ml EBM™-2 medium (Lonza, Breda, the Netherlands) supplemented with the EGM™-2 BulletKit™ (Lonza), 100 mL fetal bovine serum (Gibco®, Invitrogen, Carlsbad, CA), and 7 mL Antibiotic Antimycotic solution (Sigma-Aldrich #A5955, St. Louis, MO). Cells were seeded on 48 wells Nunc™ Cell-Culture Treated Multidishes (Nunclon, Roskilde, Denmark) pre-coated with 50 µg/mL rat tail collagen type I (BD Biosciences). Medium was refreshed every other day. Cells were passaged according to the scheme in Fig. S1A.

The study protocol was approved by the Leiden University Medical Center ethics review board. Informed consent was obtained from all subjects in accordance with the Declaration of Helsinki.

ECFC culture

ECFCs were cultured in EGM-20 culture medium, which was refreshed every other day. All experiments were performed on cells that were 3-5 days confluent. Cells were considered confluent when they stopped expanding as determined by the cell number per mm^2 (maximum cell density). Cell density was determined by the ITCN plug-in (v1.6) of Fiji, ImageJ (ImageJ 1.51r, Bethesda, MD) on bright-field images that were taken daily. Each single ECFC line at passage 5 was simultaneously subjected to fluorescence-activated cell sorting (FACS) analysis, gene expression analysis and tube formation analysis on Matrigel (Fig. S1B). Immunofluorescent staining and VWF antigen (VWF:Ag) measurements were performed in separate experiments (Fig. S1C). The characterization of each ECFC line was performed in two independent experiments, except for FACS analysis, which was performed once for each ECFC line.

FACS analysis

Surface marker expression was detected with flow cytometry. ECFCs were pelleted and washed with FACS buffer (PBS; 1% bovine serum albumin [Sigma-Aldrich]; 0.01% sodium azide) and incubated on ice for 30 minutes with the following labeled primary antibodies or

isotype controls: CD14-FITC (BD Biosciences), CD31-FITC (PECAM1; BD Biosciences), CD45-Pacific Blue (BD Biosciences), CD144-PE (VE-cadherin; R&D), CD146-PerCp-Cy5 (MCAM, BD Biosciences), IgG1-FITC (R&D), IgG1-PE (BD Biosciences), IgG1-PerCp-Cy5, and IgG1-Pacific blue (all BD Biosciences). After antibody incubation, cells were washed in FACS buffer and run on the LSRII (BD Biosciences). Data were analyzed using FACSDiVa software (BD Biosciences).

VWF:Ag measurements

Basal VWF secretion was determined by the release of VWF over 24 hours in EGM-20 culture medium. For determination of intracellular VWF, cells were lysed overnight at 4°C in Opti-MEM™ I Reduced Serum Medium (Thermo Fisher Scientific, Carlsbad, CA) containing 0.1% Triton X-100 (Sigma-Aldrich) supplemented with cOmplete™ Protease Inhibitor Cocktail with EDTA (Roche Diagnostics, Mannheim, Germany). VWF:Ag levels were measured in conditioned medium and cell lysates by ELISA as previously described.[18]

Confocal immunofluorescence microscopy

ECFCs were plated on rat tail collagen (50 µg/mL) coated glass coverslips. Three different staining procedures were used to detect intra- and/or extracellular VWF. Solely intracellular VWF was visualized after fixation and permeabilization with ice-cold methanol, after which the cells were washed twice with PBS and blocked with PBS, 1% fetal bovine serum (Gibco) and 1% bovine serum albumin (Sigma-Aldrich). Intra- as well as extracellular VWF was visualized after fixation with 4% paraformaldehyde (Alfa Aesar, Karlsruhe, Germany), after which the cells were washed once and blocked and permeabilized with PBS, 5% normal goat serum (DAKO, Glostrup, Denmark) and 0.02% saponin (Sigma-Aldrich). Extracellular VWF was visualized after fixation with 4% paraformaldehyde, after which the cells were washed once and blocked with PBS and 5% normal goat serum (DAKO). Cells were stained for VWF with polyclonal antibody rabbit anti-hVWF (A0082, DAKO) and for VE-cadherin with purified mouse anti-human CD144 (BD Biosciences) diluted in the corresponding blocking buffer. Nuclear staining was performed with Hoechst (Thermo Fisher Scientific) diluted in PBS. Coverslips were mounted by ProLong® Diamond Antifade Mountant (Thermo Fisher Scientific) and cells were visualized by the Leica TCS SP8 X WLL converted confocal microscope equipped with a HC PL APO CS2 63x/1.40 OIL immersion objective.

Matrigel tube formation

Ninety-six wells plates were coated with 46 µL/well growth factor reduced Matrigel (BD Biosciences) for 1 hour at 37°C. ECFCs were seeded on the Matrigel at a concentration of 15,000 cells per well in EGM-2 medium. The culture plate was placed in a Leica DMI6000

inverted microscope with an environmental chamber for control of temperature (37°C) and CO_2 concentration (5%). Images were taken every 15 minutes with a 10x magnification using a LEICA DF350FX CCD camera until 24 hours after seeding cells. Analyses were performed with Fiji (ImageJ) using the Angiogenesis Analyzer plugin (version 1.0c). Two independent experiments were performed in triplicate for each ECFC line. Average values of triplicates were calculated for the tube length, number of branches, and number of meshes as characteristics of each ECFC line.

Gene expression

RNA was isolated using the RNeasy Micro Kit (Qiagen, Venlo, the Netherlands). Complementary DNA was synthesized using SuperScript™ II Reverse Transcriptase (Thermo Fisher Scientific) with poly(T) primers (Sigma-Aldrich). Quantitative PCR (qPCR) was performed using Sybr™ Select Master Mix (Thermo Fisher Scientific) in the CFX384 Touch instrument (Bio-Rad, Veenendaal, the Netherlands) with *GAPDH* as endogenous reference gene. Table S1 shows sequences of gene specific primers. The comparative Ct method was used as described by Wong and Medrano.[19]

Statistics

GraphPad Prism, version 7.00 (GraphPad Software, La Jolla, CA), was used for graphics and statistical analyses. Pearson correlation was used to determine the strength of association between cell density and all other measured parameters. Significance was set at $P < 0.05$ (two-tailed).

Results

Phenotypic characterization

ECFCs were isolated from six healthy donors which resulted in the outgrowth of 16 ECFC lines. In isolations of some donors, several clones appeared and these lines were cultured separately (for example, for donor 4, these multiple clones were named ECFC line 4A, 4B, etc.), so we could study both inter- and intra-donor variability. All ECFCs were positive for endothelial markers CD31 and CD146 and negative for leukocyte markers CD14 and CD45; however, a subset of ECFC lines showed decreased positivity for CD144 suggesting a mixed population (Fig. 1A, all histograms in Fig. S2). Furthermore, remarkable differences were observed between cell sizes at maximum confluency and morphology of the different lines (Fig. 1B and Fig. S3) and we observed that cell lines with bigger cell sizes have a more mesenchymal phenotype and could reach a lower cell density at maximum confluency. These “low cell density” ECFC lines

are the lines with decreased positivity for CD144 (Fig. 1C). Because we would like to show the characteristics of all cell populations that appear after ECFC isolation, we did not exclude cells for which the ECFC identity may be less clear because of lower CD144 positivity (i.e., ECFCs 1, 2, 6A, 6C, and 6E).

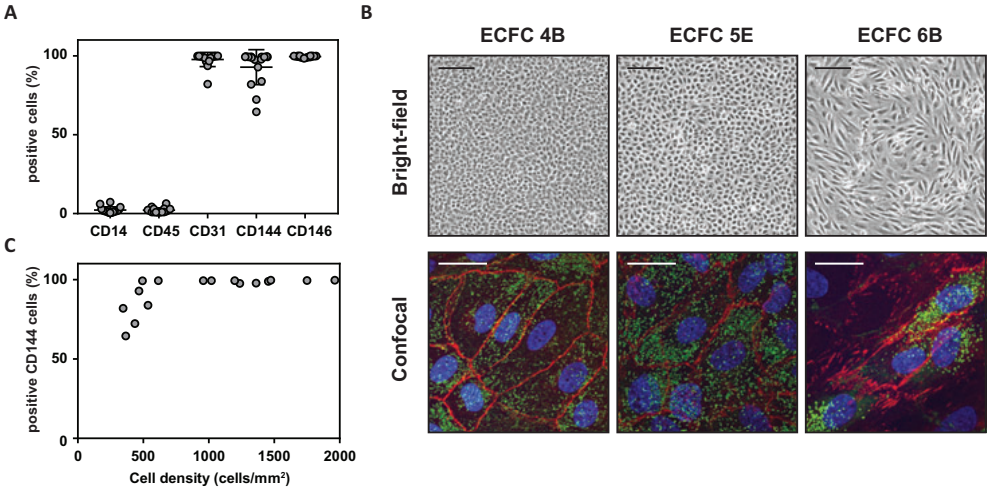

Figure 1. ECFC surface marker expression and cell morphology. (A) FACS analysis for surface markers CD14, CD31, CD45, CD144, and CD146 of all 16 ECFC lines derived from six healthy donors. All ECFC lines are negative for CD14 and CD45 and positive for CD31 and CD146. Variation is observed in CD144 expression. (B) Bright-field and confocal images of three representative ECFC lines with high, medium and low maximum cell densities 3-5 days after the cells stopped expanding. Bright-field images show clear morphological variation between ECFC lines. Scale bar in bright-field images represents 200 µm. Confocal images show VWF (green) and VE-cadherin (red). Staining patterns clearly vary between ECFC lines, with VWF in Weibel-Palade bodies more at the periphery of the cell in lines with a high maximum cell density (ECFC 4B), VWF in elongated Weibel-Palade bodies dispersed throughout the whole cell in lines with an intermediate maximum cell density (ECFC 5E), and sparse VWF and more diffuse VE-cadherin staining in lines with a low maximum cell density (ECFC 6B). Scale bar in confocal images represents 10 µm. (C) FACS analysis for CD144 in all 16 ECFC lines. Cells with a maximum cell density below 500 cells/mm^2 showed reduced positivity for CD144 (<500 cells/mm^2 81.9 (64.5-99.2); >500 cells/mm^2 99.3 (83.8-99.6), median (range), P = 0.0073, Mann-Whitney). ECFC, endothelial colony forming cell; FACS, fluorescence-activated cell sorting; VWF, von Willebrand factor

VWF:Ag measurements

To evaluate the optimal timepoint to perform experiments, seven proliferative ECFC lines were subconfluently plated and followed over time for secreted VWF:Ag levels and cell density (bright-field images of three representative cell lines in Fig. S4). Maximum VWF:Ag levels were measured in conditioned medium 3-5 days after the ECFCs stopped expanding (maximum cell density). Both secreted VWF:Ag levels, and cell density remained constant after the maximum density was reached (Fig. 2A); therefore, all experiments in this study were performed at this stable phase, 3-5 days after the cells stopped expanding. The results for VWF secretion and cell density were comparable to observations in HUVECs.[20,21]

To determine differences in VWF:Ag secretion between the different ECFC lines, VWF:Ag levels released in 24 hours were measured in conditioned medium at maximum cell density. Interestingly, we observed a significant correlation between secreted VWF:Ag levels and maximum cell density, where cell lines with a high maximum cell density secreted more VWF than lines with a low maximum cell density ($R^2 = 0.89$, $P = 0.0001$; Fig. 2B). A correlation between secreted VWF:Ag levels and cell density is also observed in the days before maximum cell density; however, the slope of the lines is lower and increases until the day we measure highest VWF:Ag level. This slope remained constant from that moment on, just as the VWF:Ag levels did (data not shown). All separate clones were analyzed as independent data points, but a significant correlation between VWF:Ag secretion and maximum cell density was still present when all clones of a single donor were pooled. ECFC lines with a maximum cell density below 500 cells/mm^2 (ECFCs 1, 2, and 6A-E) had a VWF:Ag secretion below the lower limit of detection and were therefore excluded in the correlation analysis. The fold increase of VWF release in 1 hour after histamine stimulation over the release in 1 hour in unstimulated cells (the stimulation factor) was similar for all cell lines and was not related to maximum cell density (data not shown).

To exclude that cells with a high maximum cell density have a higher secretion rate and therefore lower intracellular VWF:Ag levels, we measured total VWF:Ag levels in conditioned medium and cell lysates. However, total VWF:Ag production also significantly correlated with maximum cell density ($R^2 = 0.96$, $P < 0.0001$; Fig. 2C). Because the total VWF:Ag level per individual cell was also higher in smaller cells, we excluded that higher VWF:Ag levels were measured because of the presence of a higher number of cells (Fig. 2D). Also, on the mRNA level, a significant correlation was observed between maximum cell density and *VWF* ($R^2 = 0.63$, $P = 0.0002$; Fig. 2E). Different clones that were isolated from individual donors also show variations in maximum cell density (Fig. 2F) and VWF:Ag expression (Fig. 2G) and we therefore subsequently analyzed all ECFC lines as individual clones.

Passaging of endothelial cells can result in morphological changes[22]; therefore, maximum cell density and VWF:Ag secretion at increasing passage numbers were studied. Two ECFC lines (4B and 5A) were passaged until they stopped proliferating at passage number 15 and 12, respectively. Both lines showed a decrease in maximum cell density with increasing passage number, which correlated with decreased secreted VWF:Ag levels (Fig. 2H and I). Furthermore, the ECFC line with the highest maximum cell density (4B) could be passaged until a higher passage number compared to the ECFC line with a lower maximum cell density (5A).

Overall, VWF production correlate with maximum ECFC density. This is observed both in cells at similar passage numbers and in cells with increasing passage numbers.

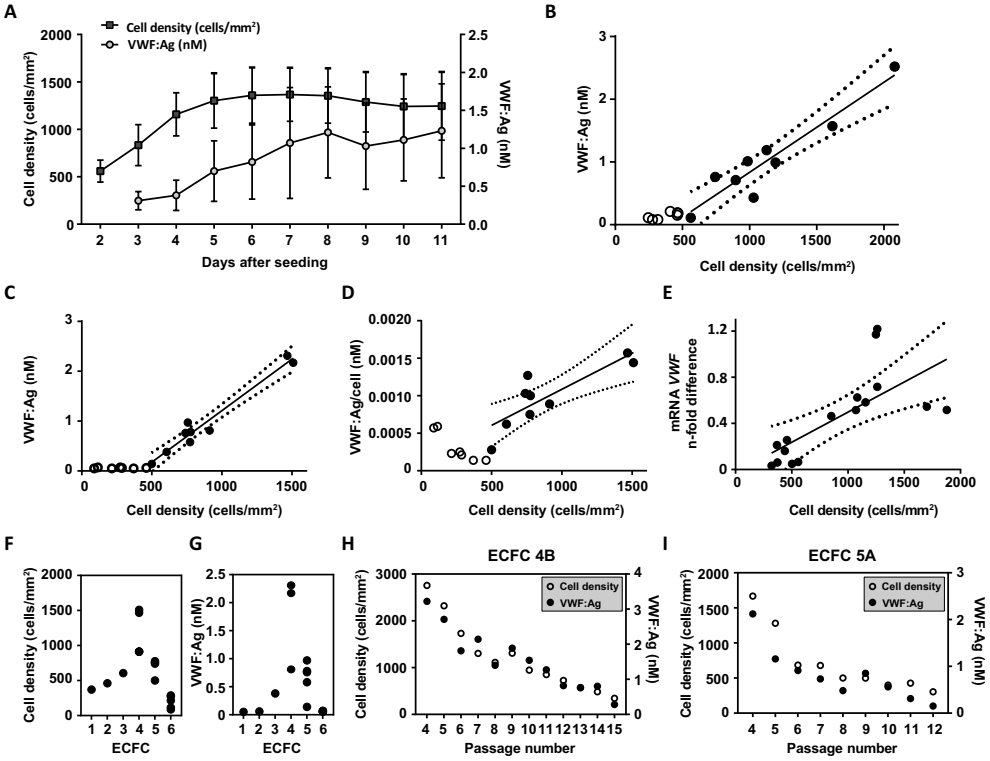

Figure 2. VWF quantification and its relation to cell density. (A) Average cell density and secreted VWF:Ag levels measured in conditioned medium that was harvested and refreshed every 24 hours in seven subconfluently plated ECFC lines. Highest VWF:Ag levels were identified 3-5 days after the cells stopped expanding. Both cell density and VWF:Ag production remained constant after the maximum was reached. (B) Secreted VWF:Ag levels measured in conditioned medium 24 hours after refreshing the medium showed a significant correlation with maximum cell density of ECFC lines with a maximum cell density of more than 500 cells/mm^2 (R^2 = 0.89, P = 0.0001). Open circles: maximum cell density <500 cells/mm^2; closed circles: maximum cell density >500 cells/mm^2. Each data point represents the average of two independent experiments. (C) Total VWF:Ag levels measured in conditioned medium and cell lysates 24 hours after refreshing the medium significantly correlate with maximum cell density of ECFC lines with a maximum cell density of more than 500 cells/mm^2 (R^2 = 0.96, P < 0.0001). Open circles: maximum cell density <500 cells/mm^2; closed circles: maximum cell density >500 cells/mm2. (D) Total VWF:Ag levels per cell measured in conditioned medium and cell lysates 24 hours after refreshing the medium significantly correlate with maximum cell density of ECFC lines with a maximum cell density of more than 500 cells/mm^2 (R^2 = 0.71, P = 0.0045). Open circles: maximum cell density <500 cells/mm^2; closed circles: maximum cell density >500 cells/mm^2. (E) *VWF* mRNA levels measured by qPCR significantly correlate with maximum cell density (R^2 = 0.63, P = 0.0002). (F) Different ECFC lines per donor show variable cell densities at maximum confluency (G) Different ECFC lines per donor show variable VWF:Ag levels. (H) and (I) Maximum cell density and secreted VWF:Ag levels measured in conditioned medium 24 hours after refreshing the medium decrease with increasing passage number for ECFC lines 4B (H) and 5A (I). ECFC, endothelial colony forming cell; VWF, von Willebrand factor

VWF localization

Endothelial cells store VWF in Weibel-Palade bodies.[3] To investigate whether the ECFC lines were able to store VWF in Weibel-Palade bodies, all ECFC lines were stained for VWF and endothelial marker VE-cadherin. Although all ECFC lines showed VWF in Weibel-Palade bodies,

large differences were observed in staining patterns (Fig. 1B for representative examples, all data in Fig. S3). ECFC lines with a very high maximum cell density (4A and 4B) showed mainly VWF staining closer to the cell membrane. Also, strings of released VWF were observed in some of these cell lines, whereas the cells were not extrinsically stimulated to secrete VWF (Fig. S3, stainings with PFA fixation). Cells with an intermediate maximum cell density and VWF production showed VWF staining in typical elongated Weibel-Palade bodies dispersed throughout the cell. Cells with a low maximum cell density showed only sparse VWF staining in a subset of cells. Interestingly, some ECFC lines with a low maximum cell density showed reduced VE-cadherin staining. This was in line with FACS results where cells with a maximum cell density below 500 cells/mm^2 showed decreased positivity for CD144 (Fig. 1B and C).

Matrigel tube formation

Compared with the normal population, an increased number of VWD patients suffer from intestinal bleeding caused by angiodysplasia.[23] Several studies have shown a negative correlation of VWF and angiogenesis and VWF downregulation in an *in vitro* small interfering RNA knockdown assay resulted in increased angiogenic capacity.[12,13,24] We therefore reasoned that ECFC lines with low VWF production might have higher angiogenic potential than ECFC lines with high VWF production.[24]

The angiogenic properties of all 16 ECFC lines were investigated in an *in vitro* Matrigel tube formation assay. Herewith, the ability of endothelial cells to form tube-like structures was investigated, involving endothelial cell adhesion and migration. The formation of tube-like structures of all ECFC lines was followed for 24 hours. Although the angiogenic capacity clearly differed between ECFC lines (Fig. S3), the maximum tube length (Fig. 3A) and maximum number of branches, meshes, and junctions (data not shown) were mostly reached between 2 and 6 hours after seeding the cells. After maximum levels were reached, the cells migrated to form cell clumps for low maximum cell density ECFC lines or structures were destroyed in case of high maximum cell density ECFC lines; therefore, we used the average of the maximum value and the four adjacent values of each parameter in all analyses. Significant correlations with maximum cell density and maximum tube length ($R^2 = 0.72$, $P < 0.0001$; Fig. 3B), maximum number of meshes ($R^2 = 0.60$, $P < 0.001$; Fig. 3C) and maximum number of branches ($R^2 = 0.75$, $P < 0.0001$; Fig. 3D) were observed. Overall, the maximum cell density of ECFCs show a negative correlation with the angiogenic capacity.

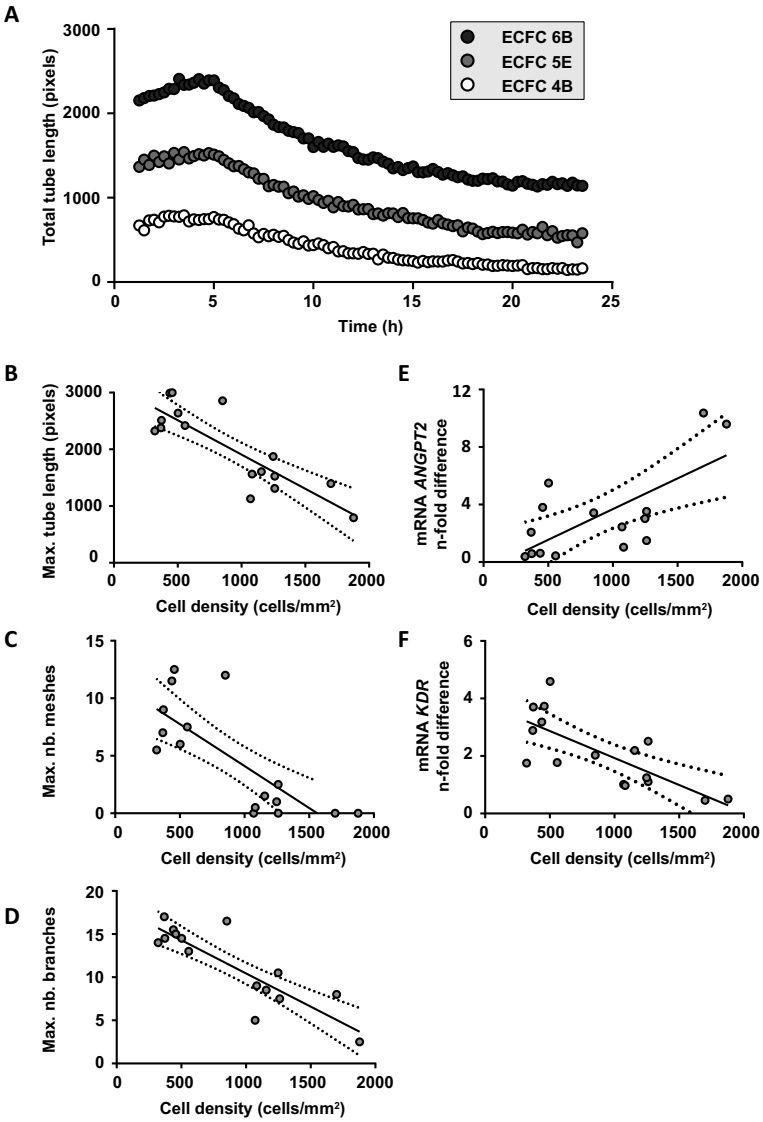

Figure 3. Angiogenesis potential of ECFC lines and its relation to maximum cell density. (A) The ability of ECFC lines to form tubes on Matrigel was followed for 24 hours. Plotted are the total tube length for three ECFC lines representative for low (ECFC 6B), medium (ECFC 5E), and high (ECFC 4B) maximum cell density. The maximum tube length was measured by the Angiogenesis Analyzer plugin of Fiji (ImageJ) and maximum tube length was reached between 2 and 6 hours after plating the cells. Highest tube length was observed in ECFC lines with a low maximum cell density. (B) The maximum tube length and the maximum number of (C) meshes and (D) branches that were measured in 24 hours were plotted against maximum cell density. Maximum tube length ($R^2 = 0.72$, $P < 0.0001$) and maximum number of meshes ($R^2 = 0.60$, $P < 0.001$) and branches ($R^2 = 0.75$, $P < 0.0001$) significantly correlated with maximum cell density. (E) Gene expression analysis of *ANGPT2* showed a significant positive correlation with maximum cell density ($R^2 = 0.42$, $P < 0.01$). (F) gene expression analysis of *KDR* showed a significant negative correlation with maximum cell density ($R^2 = 0.66$, $P = 0.0001$). (A-F) Each data point represents the average of two independent experiments. ANGPT2, Angiopoeitin-2; ECFC, endothelial colony forming cell; KDR, vascular endothelial growth factor receptor 2; VWF, von Willebrand factor

Gene expression of the angiogenic markers angiopoietin-2 (*ANGPT2*), *CD34*, *CD105* (endoglin), and VEGF receptor-2 (or kinase insert domain receptor, *KDR*) was evaluated to investigate the underlying mechanism for the observed variations. No correlation was detected between maximum cell density and *CD34* or *CD105* expression (data not shown). Interestingly, *ANGPT2* (R^2 = 0.42, P < 0.01; Fig. 3E) and *KDR* (R^2 = 0.66, P = 0.0001; Fig. 3F) expression significantly correlated with maximum cell densities, with higher levels of *ANGPT2* in cell lines with high maximum cell densities and higher levels of *KDR* in lines with lower maximum cell densities.

Gene expression of aging and endothelial to mesenchymal transition markers

Gene expression analysis was performed on several pathways to better understand the mechanisms behind the variations between ECFC lines. Because passaging of cells resulted in decreased maximum cell density and lower VWF:Ag production (Fig. 2H and I), we reasoned that aging (cellular senescence) might underlie the observed variations. This was tested by gene expression analysis of SRY-Box 18 (*SOX18*) and C-X-C Motif Chemokine Ligand 8 (*CXCL8*). *SOX18* is described to be higher in early passage ECFCs, whereas *CXCL8* is higher in ECFCs close to their Hayflick limit.[22] *CXCL8* is also described as a modulator of senescence, and its gene expression significantly correlates with β-galactosidase and γH2AX stainings.[22] We confirm the influence of aging on the variations seen in the ECFC lines by significant correlations between maximum cell density and gene expression of *CXCL8* (R^2 = 0.84, P < 0.0001; Fig. 4A) and *SOX18* (R^2 = 0.79, P < 0.0001; Fig. 4B). A lower expression of *CXCL8* and a higher expression of *SOX18* was detected in lines with a high maximum cell density. The inverse was true for lines with a low maximum cell density.

ECFC lines with a lower maximum cell density showed loss of cell-cell interactions and loss of the typical cobblestone morphology, observations that correlate with a mesenchymal-like phenotype. Transition of endothelial cells to a more mesenchymal phenotype is described as endothelial to mesenchymal transition (EndoMT). In EndoMT, gene expression of endothelial markers is reduced, whereas an induction in expression of extracellular matrix proteins becomes apparent.[25,26] We observed significant negative correlations between maximum cell density and mesenchymal marker α-smooth muscle actin (*ACTA1*, R^2 = 0.81, P < 0.0001; Fig. 4C) and significant positive correlations between maximum cell density and endothelial basement membrane protein vimentin (*VIM*, R^2 = 0.59, P < 0.001; Fig. 4D). Collagen Type I Alpha 1 Chain (*COL1A1*; Fig. 4E) showed especially high expression levels in cell lines with a low maximum cell density (<500 cells/mm^2). Increased EndoMT could be the result of increased shear stress, and although our cells are cultured under static conditions, we investigated gene expression of known shear stress markers Krüppel Like Factor 2 (*KLF2*) and Ephrin B2 (*EFNB2*) as well as KLF2 downstream target thrombomodulin (*THBD*). Interestingly, ECFC density

significantly correlated with *KLF2* gene expression ($R^2 = 0.79$, $P < 0.0001$; Fig. 4F), wherein ECFC lines with smaller cells expressed higher levels of KLF2. The same was true when correlating ECFC density with *EFNB2* ($R^2 = 0.86$, $P < 0.0001$; Fig. 4G) and *THBD* ($R^2 = 0.82$, $P < 0.0001$; Fig. 4H).

Overall, gene expression of senescence and EndoMT markers negatively correlate with ECFC density, whereas shear stress markers positively correlate with ECFC density.

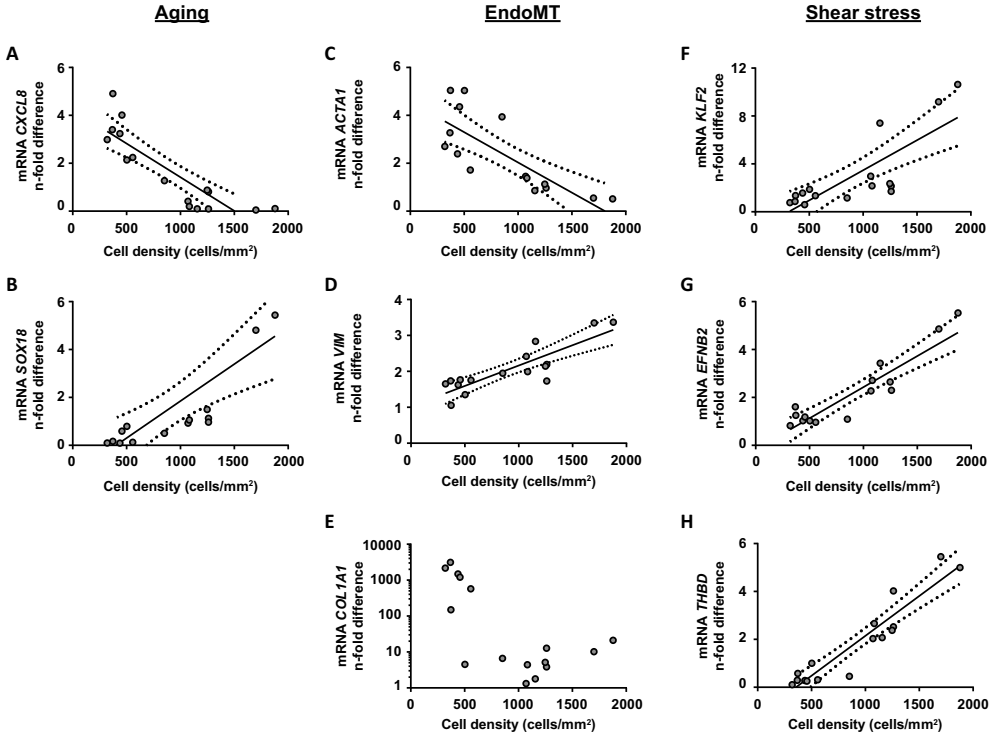

Figure 4. ECFC gene expression analysis on genes related to aging, EndoMT and shear stress. (A) Gene expression analysis of aging marker *CXCL8* show a negative correlation with maximum cell density ($R^2 = 0.84$, $P < 0.0001$). (B) Gene expression analysis of aging marker *SOX18* show a positive correlation with maximum cell density ($R^2 = 0.79$, $P < 0.0001$). (C) Gene expression analysis of EndoMT marker *ACTA1* show a negative correlation with maximum cell density ($R^2 = 0.81$, $P < 0.0001$). (D) Gene expression analysis of EndoMT marker *VIM* show a positive correlation with maximum cell density ($R^2 = 0.59$, $P < 0.001$). (E) Gene expression analysis of EndoMT marker *COL1A1* is strongly increased in cell lines with a low maximum cell density. (F) Gene expression analysis of shear stress marker *KLF2* shows a positive correlation with maximum cell density ($R^2 = 0.79$, $P < 0.0001$). (G) Gene expression analysis of shear stress marker *EFNB2* shows a positive correlation with maximum cell density ($R^2 = 0.86$, $P < 0.0001$). (H) Gene expression analysis of *THBD*, a downstream target of KLF2, shows a positive correlation with maximum cell density ($R^2 = 0.82$, $P < 0.0001$). (A-H) Each data point represents the average of two independent experiments. ACTA1, alpha smooth muscle actin; CXCL8, C-X-C Motif Chemokine Ligand 8; EFNB2, Ephrin B2; EndoMT, endothelial to mesenchymal transition; COL1A1, collagen Type 1 Alpha 1 Chain; KLF2, Krüppel-like Factor 2; SOX18, SRY-Box 18; THBD, Thrombomodulin; VIM, vimentin

Discussion

ECFCs have been used in the past years to study pathophysiological effects of VWF mutations on a cellular level. Although knowledge on VWD pathophysiology has been improved by the use of ECFCs, high variations in ECFC morphology, VWF expression, and several other VWF-related parameters cannot be neglected. We have therefore studied the extent of variations in maximum cell density, VWF expression, VWF storage, and the capacity of ECFCs to form tubes on Matrigel in 16 ECFC lines derived from six healthy donors. Furthermore, we evaluated the mechanisms that could explain the variations by gene expression evaluation in the same set of ECFCs.

Although all ECFC lines used in this study were positive for endothelial markers CD31 and CD146 and negative for leukocyte markers CD14 and CD45, variations were observed in CD144 expression profile and the morphology of different ECFC lines. Especially cell density at maximum confluency was markedly different between the lines and this maximum cell density positively correlated with VWF production. Because maximum cell density correlates with VWF production (Fig. 2B-E), deviations from this line might indicate defective VWF secretion caused by, for example, retention in endoplasmic reticulum or Golgi. As a measure for cell density, we counted the cell number in bright-field images taken from the ECFCs immediately before performing the experiments. Although this is not a conventional method, this method does reflect the conditions at the moment of the experiment itself. Where cell count after trypsinization only informs on the cell count before plating the cells. However, cell count after trypsinization does correlate with cell count by ImageJ. In ECFC lines with a very low maximum cell density, we could not detect VWF by ELISA. We did not exclude these cells from most analyses because we aimed to show the characteristics of all cell lines that appear after the isolation procedure. However, it is questionable whether cells with a maximum cell density <500 cells/mm^2 and decreased CD144 expression are true endothelial cells (even though these cells are CD14 and CD45 negative and CD31 and CD146 positive) or are a mixed population. We therefore suggest, based on the results shown in this study, not to use these cells in VWF/VWD research. However, when studying specific patients with a unique clinical phenotype, one may have to accept that the patient-derived ECFCs have a mixed phenotype. When “suboptimal” patient-derived clones with a mixed phenotype appear, it is then of utmost importance to compare these cell lines with an appropriate, and if necessary a mixed control.

The effects of passaging of ECFCs was determined in two ECFC lines and we observed a decrease in maximum cell density and VWF production every time a cell line was passaged. Furthermore, the ECFC line with the smallest cells and therefore highest maximum cell density (ECFC 4B) could reach a higher passage number than the ECFC line with the bigger cells and lower maximum cell density (ECFC 5A). The passage number indicates the number of times a cell line has been trypsinized and subcultured (Fig. S1), but is not to be confused

with the population doubling level, which is the number of times a cell has doubled since the primary isolation. Because ECFC 4B has a higher maximum cell density than ECFC 5A, the exact number of cell doublings that can be reached for ECFC 4B is even higher than the passage number indicates compared with ECFC 5A. Furthermore, passaging of cells also led to decreased maximum cell density and VWF production, which indicates that one single ECFC line can have different cellular characteristics.

An increased percentage of VWD patients compared to the normal population develop intestinal bleeding caused by angiodysplasia.[27] This is the result of increased angiogenesis, a process that *in vitro* can be simulated by a Matrigel tube formation assay. Although ECFCs proved to be a strong tool to study angiogenesis *ex vivo*, the exact role of VWF in angiogenesis remains unclear. Most importantly, small interfering RNA-mediated downregulation of VWF in HUVECs led to increased Matrigel tube formation.[24] We showed clear variations in angiogenic capacity between healthy control ECFCs with increased angiogenic capacity in lines with low VWF production compared with lines with high VWF production. It is important to acknowledge these inter-clonal variations in healthy control ECFCs, especially when drawing conclusions on patient-derived ECFCs. We showed decreased VWF production in cells with increased passage number, which might suggest that ECFCs at higher passage numbers show increased tube formation. This was however not observed by Groeneveld *et al*, where reduced tube formation was observed in late passage cells.[12] This indicates that other cell characteristics in aged cells are more important in *ex vivo* tube formation than VWF itself. One important remark is that ECFCs with a low maximum cell density have a bigger cell diameter upon seeding on Matrigel, compared with lines with a high maximum cell density; therefore, the distance between cells was smaller, which might affect tube formation. Different types of assays in which tube formation is followed from a monolayer of cells might give better insight in the angiogenic capacity of ECFCs.[28,29] But with these results, we address the presence of variations between ECFC lines on angiogenic potential. Several angiogenic markers that could explain the variations were measured by qPCR. Most important, we observed a significant correlation for maximum cell density and *KDR* with increased *KDR* expression in lines with a low maximum cell density. KDR is known to promote angiogenesis, which is in line with the observations seen in the studied ECFCs.

Variations between ECFC lines were observed in VWF production and tube formation on Matrigel. To understand the cause of the variations, we measured the expression of genes involved in two processes that might underlie these variations: aging and endoMT. Because cells age and increase in cell size with each passage number and ECFC lines with a high maximum cell density could reach a higher passage number, we reasoned that low maximum cell density ECFC lines are in a more senescent state than high maximum cell density ECFC lines, irrespective of the passage number or cell doubling level. Indeed, we found a significant

correlation between maximum cell density and senescence markers *CXCL8* and *SOX18*, suggesting that cell lines with a low maximum cell density are more senescent than cells with a high maximum cell density. This is an interesting observation because ECFCs with a low maximum cell density have bigger cells and therefore had less cell doublings in culture than ECFC lines with a high maximum cell density at the same passage number. A possible explanation could be that the cells from which the ECFC lines originate vary in their senescent state or that the cells have a different origin (i.e., tissue-specific or bone-marrow derived); however, more research is necessary to confirm this.[30] Although more markers are needed to fully define senescence, we highlight with these markers differences between cell lines.

EndoMT was studied as possible explanation for the variations because low maximum cell density lines had a more mesenchymal phenotype with loss in cell-cell contacts. We confirmed a more mesenchymal phenotype in low-density lines by gene expression analysis of mesenchymal markers *ACTA1*, *VIM*, and *COL1A1*. EndoMT could be induced by shear stress[31] and although all experiments are performed under static conditions, increased expression of shear stress markers *KLF2* and *EFNB2* was observed in high maximum cell density lines. This does not explain the mesenchymal phenotype observed in low maximum cell density lines, but opened up a possible different mechanism. The transcription factor KLF2 is also described as transcriptional switch between quiescent and activated endothelial cells.[32] This suggests that cells from high maximum cell density lines are in a more activated state, which might explain the secreted VWF strings observed in immunofluorescent stainings of these lines. *VWF* and Thrombomodulin are both under the expression of KLF2 and are both upregulated in high maximum cell density lines.

To conclude, we observed variations in morphology, maximum cell density, VWF:Ag production, and angiogenic capacity in ECFCs from healthy controls. And ECFC lines with a low maximum cell density are suggestive for a mixed population with a more mesenchymal cellular phenotype. The variations seem to be attributed to aging and endoMT; however, it remains unclear what exactly drives the variations in aging and endoMT. When investigating patient-derived ECFCs, these variations should always be acknowledged. Although clear variations are observed, we think that ECFCs maintain a powerful tool, especially when different conditions within one ECFC line are studied. When comparing patient-derived and control ECFCs, we suggest using cells with the same characteristics. Because there are limits to the clones that appear in patient-derived cells, it is suggested to have a large panel of healthy control ECFCs to match patient-derived ECFCs with control ECFCs. Also, it is important to take maximum cell density into account and to perform experiments 3-5 days after the cells stop expanding. We also suggest synchronization and standardization of the experiments between laboratories to fairly compare results. This is especially a necessity when sample sizes are small as they are in VWD research.

Acknowledgements

This study was financially supported by a research grant from the Landsteiner Foundation for Blood Transfusion Research (grant 1504) and by a research grant from CSL Behring.

References

1. Randi AM, Laffan MA. Von Willebrand factor and angiogenesis: basic and applied issues. *J Thromb Haemost*. 2017;**15**(1):13-20.
2. Leebeek FWG, Eikenboom JCJ. Von Willebrand's Disease. *N Engl J Med*. 2016;**375**(21):2067-2080.
3. Valentijn KM, Sadler JE, Valentijn JA, Voorberg J, Eikenboom J. Functional architecture of Weibel-Palade bodies. *Blood*. 2011;**117**(19):5033-5043.
4. McGrath RT, McRae E, Smith OP, O'Donnell JS. Platelet von Willebrand factor--structure, function and biological importance. *Br J Haematol*. 2010;**148**(6):834-843.
5. Wang JW, Groeneveld DJ, Cosemans G, et al. Biogenesis of Weibel-Palade bodies in von Willebrand's disease variants with impaired von Willebrand factor intrachain or interchain disulfide bond formation. *Haematologica*. 2012;**97**(6):859-866.
6. de Jong A, Eikenboom J. Von Willebrand disease mutation spectrum and associated mutation mechanisms. *Thromb Res*. 2017;**159**:65-75.
7. Ingram DA, Mead LE, Tanaka H, et al. Identification of a novel hierarchy of endothelial progenitor cells using human peripheral and umbilical cord blood. *Blood*. 2004;**104**(9):2752-2760.
8. Hirschi KK, Ingram DA, Yoder MC. Assessing identity, phenotype, and fate of endothelial progenitor cells. *Arterioscler Thromb Vasc Biol*. 2008;**28**(9):1584-1595.
9. Medina RJ, Barber CL, Sabatier F, et al. Endothelial Progenitors: A Consensus Statement on Nomenclature. *Stem Cells Transl Med*. 2017;**6**(5):1316-1320.
10. Starke RD, Paschalaki KE, Dyer CE, et al. Cellular and molecular basis of von Willebrand disease: studies on blood outgrowth endothelial cells. *Blood*. 2013;**121**(14):2773-2784.
11. Wang JW, Bouwens EA, Pintao MC, et al. Analysis of the storage and secretion of von Willebrand factor in blood outgrowth endothelial cells derived from patients with von Willebrand disease. *Blood*. 2013;**121**(14):2762-2772.
12. Groeneveld DJ, van Bekkum T, Dirven RJ, et al. Angiogenic characteristics of blood outgrowth endothelial cells from patients with von Willebrand disease. *J Thromb Haemost*. 2015;**13**(10):1854-1866.
13. Selvam SN, Casey LJ, Bowman ML, et al. Abnormal angiogenesis in blood outgrowth endothelial cells derived from von Willebrand disease patients. *Blood Coagul Fibrinolysis*. 2017;**28**(7):521-533.
14. Hawke L, Bowman ML, Poon MC, Scully MF, Rivard GE, James PD. Characterization of aberrant splicing of von Willebrand factor in von Willebrand disease: an underrecognized mechanism. *Blood*. 2016;**128**(4):584-593.
15. Bowman ML, Pluthero FG, Tuttle A, et al. Discrepant platelet and plasma von Willebrand factor in von Willebrand disease patients with p.Pro2808Leufs*24. *J Thromb Haemost*. 2017;**15**(7):1403-1411.
16. Sadler JE. von Willebrand factor in its native environment. *Blood*. 2013;**121**(14):2583-2584.
17. Martin-Ramirez J, Hofman M, van den Biggelaar M, Hebbel RP, Voorberg J. Establishment of outgrowth endothelial cells from peripheral blood. *Nat Protoc*. 2012;**7**(9):1709-1715.

18. de Jong A, Dirven RJ, Oud JA, Tio D, van Vlijmen BJM, Eikenboom J. Correction of a dominant-negative von Willebrand factor multimerization defect by small interfering RNA-mediated allele-specific inhibition of mutant von Willebrand factor. *J Thromb Haemost*. 2018;**16**(7):1357-1368.
19. Wong ML, Medrano JF. Real-time PCR for mRNA quantitation. *Biotechniques*. 2005;**39**(1):75-85.
20. Howell GJ, Herbert SP, Smith JM, et al. Endothelial cell confluence regulates Weibel-Palade body formation. *Mol Membr Biol*. 2004;**21**(6):413-421.
21. Shahani T, Lavend'homme R, Luttun A, Saint-Remy JM, Peerlinck K, Jacquemin M. Activation of human endothelial cells from specific vascular beds induces the release of a FVIII storage pool. *Blood*. 2010;**115**(23):4902-4909.
22. Medina RJ, O'Neill CL, O'Doherty TM, et al. Ex vivo expansion of human outgrowth endothelial cells leads to IL-8-mediated replicative senescence and impaired vasoreparative function. *Stem Cells*. 2013;**31**(8):1657-1668.
23. Selvam S, James P. Angiodysplasia in von Willebrand Disease: Understanding the Clinical and Basic Science. *Semin Thromb Hemost*. 2017;**43**(6):572-580.
24. Starke RD, Ferraro F, Paschalaki KE, et al. Endothelial von Willebrand factor regulates angiogenesis. *Blood*. 2011;**117**(3):1071-1080.
25. Kalluri R, Weinberg RA. The basics of epithelial-mesenchymal transition. *J Clin Invest*. 2009;**119**(6):1420-1428.
26. Maleszewska M, Moonen JR, Huijkman N, van de Sluis B, Krenning G, Harmsen MC. IL-1beta and TGFbeta2 synergistically induce endothelial to mesenchymal transition in an NFkappaB-dependent manner. *Immunobiology*. 2013;**218**(4):443-454.
27. Castaman G, Federici AB, Tosetto A, et al. Different bleeding risk in type 2A and 2M von Willebrand disease: a 2-year prospective study in 107 patients. *J Thromb Haemost*. 2012;**10**(4):632-638.
28. Lopez JA, Zheng Y. Synthetic microvessels. *J Thromb Haemost*. 2013;**11 Suppl 1**:67-74.
29. van Duinen V, Zhu D, Ramakers C, van Zonneveld AJ, Vulto P, Hankemeier T. Perfused 3D angiogenic sprouting in a high-throughput in vitro platform. *Angiogenesis*. 2018;**22**(1):157-165.
30. Tura O, Skinner EM, Barclay GR, et al. Late outgrowth endothelial cells resemble mature endothelial cells and are not derived from bone marrow. *Stem Cells*. 2013;**31**(2):338-348.
31. Mahmoud MM, Serbanovic-Canic J, Feng S, et al. Shear stress induces endothelial-to-mesenchymal transition via the transcription factor Snail. *Sci Rep*. 2017;**7**(1):3375.
32. Dekker RJ, Boon RA, Rondaij MG, et al. KLF2 provokes a gene expression pattern that establishes functional quiescent differentiation of the endothelium. *Blood*. 2006;**107**(11):4354-4363.

Supplemental data
Figure S1

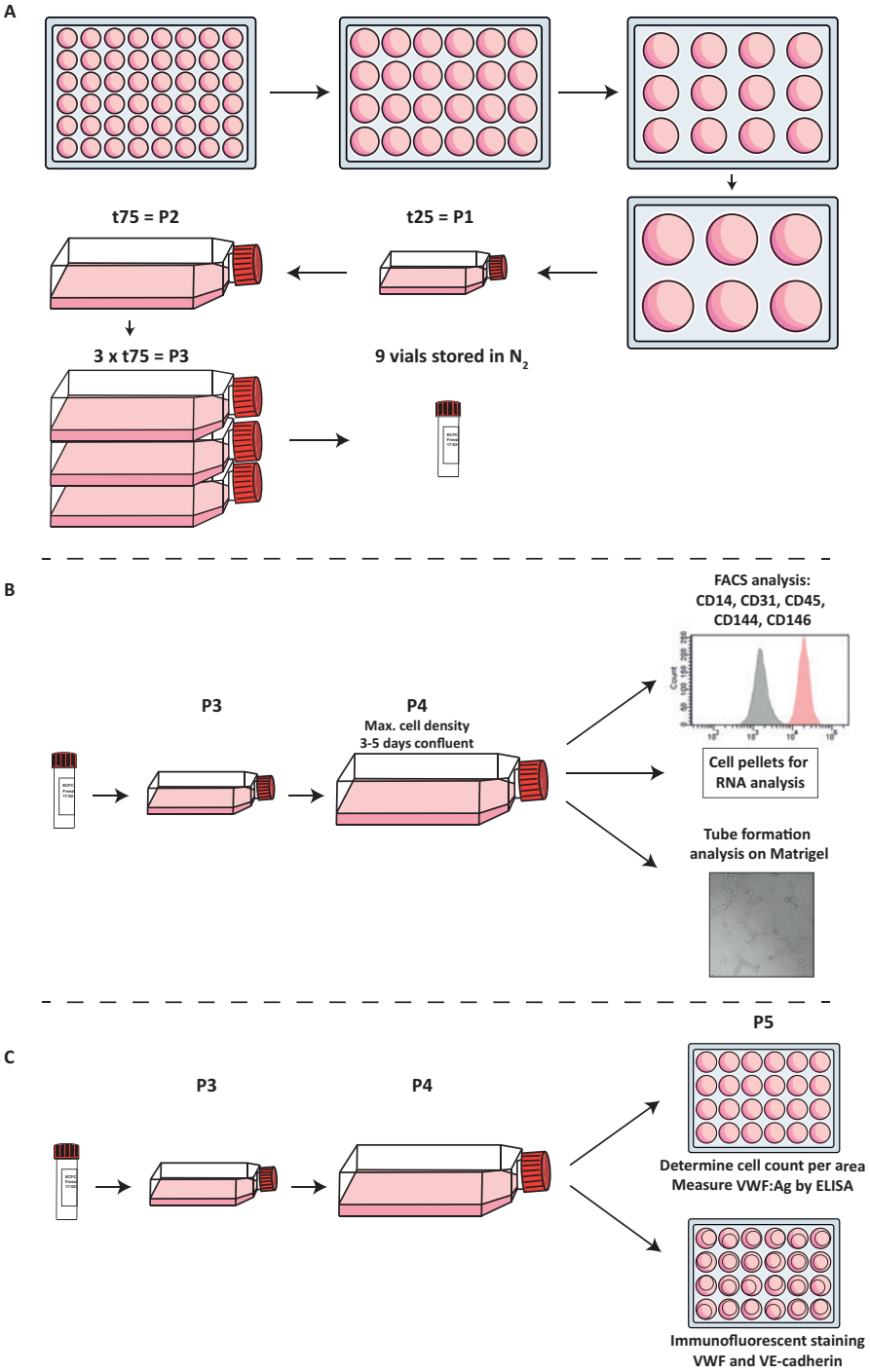

Figure S1. Schematic overview of the experimental setup. (A) peripheral blood mononuclear cells were plated in collagen coated 48 wells plates. ECFC lines appeared between days 13 and 27 after seeding. Individual lines were passaged from the 48 wells plate, to a 24 wells plate etc. Cells in a t25 culture flask where considered passage (P) 1 and cells were stored in nitrogen at P3. (B) Cells from the nitrogen storage were plated in a collagen coated t25 flask and passaged to a t75 flask. Bright-field images were taken every day and the number of cells in the images were determined by the ITCN plug-in of Fiji. Three to five days after the cells stopped expanding, cells were simultaneous subjected to FACS analysis, *in vitro* tube formation and gene expression analysis. (C) Cells from the nitrogen storage were plated in a collagen coated t25 flask and passaged to a t75 flask. From the t75 flask, cells were plated in 24 wells plates with or without coverslips. Bright-field images were taken every day from the 24 wells plates and the number of cells in the images was determined by the ITCN plug-in of Fiji. Three to five days after the cells stopped expanding, conditioned medium and protein lysates were harvested for VWF:Ag measurements and the coverslips were fixed and stained for VWF and VE-cadherin. ECFC, endothelial colony forming cell; FACS, fluorescence-activated cell sorting; VWF, von Willebrand factor

Figure S2

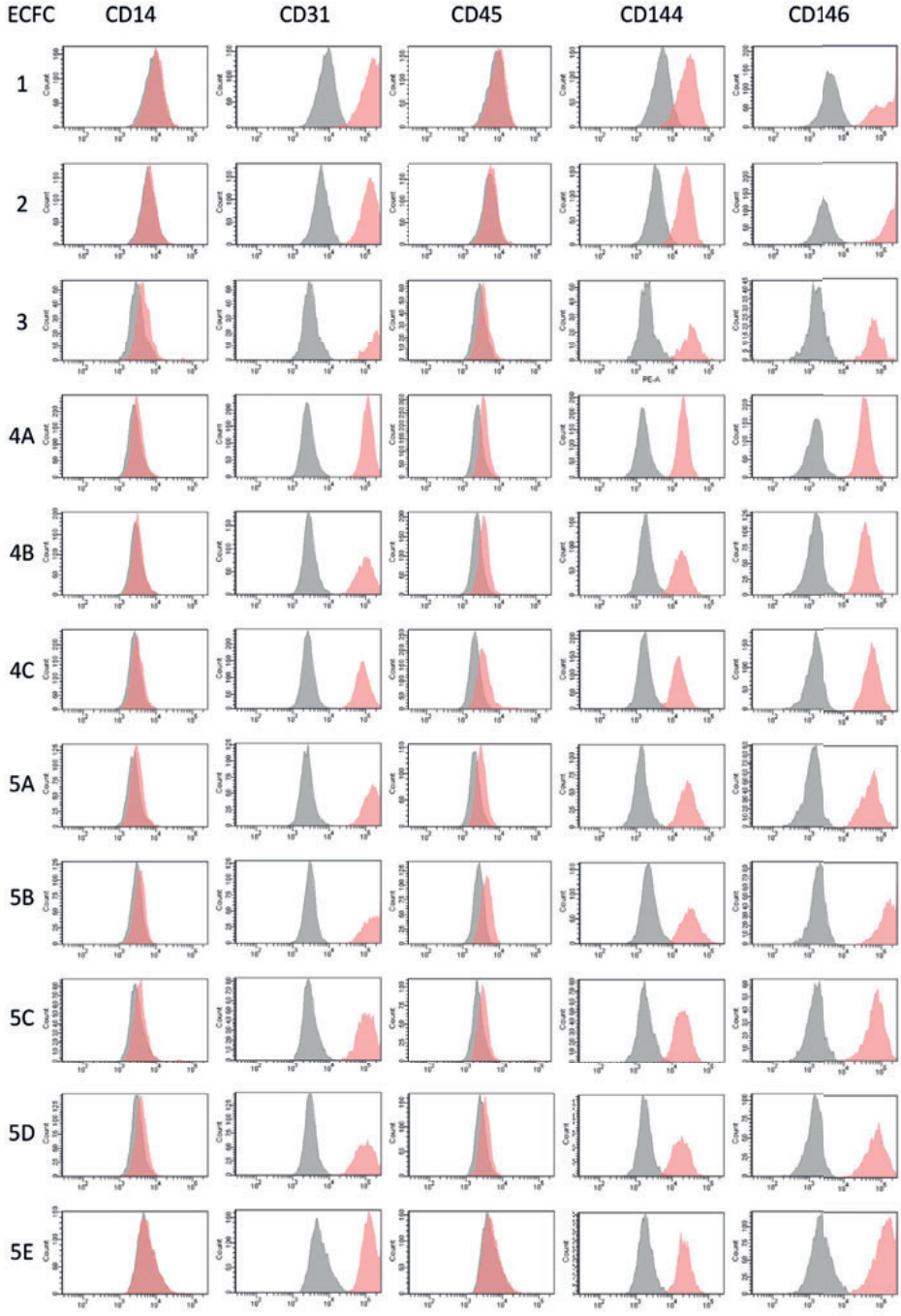
ECFC
CD14
CD31
CD45
CD144
CD146
1
2
3
4A
4B
4C
5A
5B
5C
5D
5E
Count
PE-A

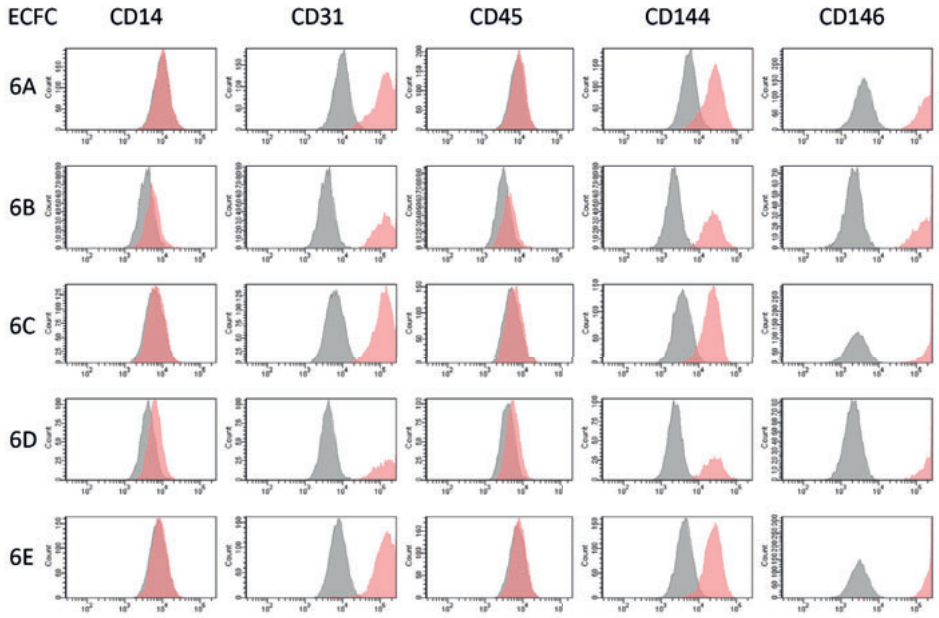

Figure S2. FACS analysis histograms of CD14, CD31, CD45, CD144 and CD146. FACS analysis for surface markers CD14, CD31, CD45, CD144 and CD146 of all 16 ECFC lines derived from six healthy donors. All ECFC lines are negative for CD14 and CD45 and positive for CD31 and CD146. Some ECFC lines have decreased positivity for CD144. ECFC, endothelial colony forming cell; FACS, fluorescence-activated cell sorting

Figure S3

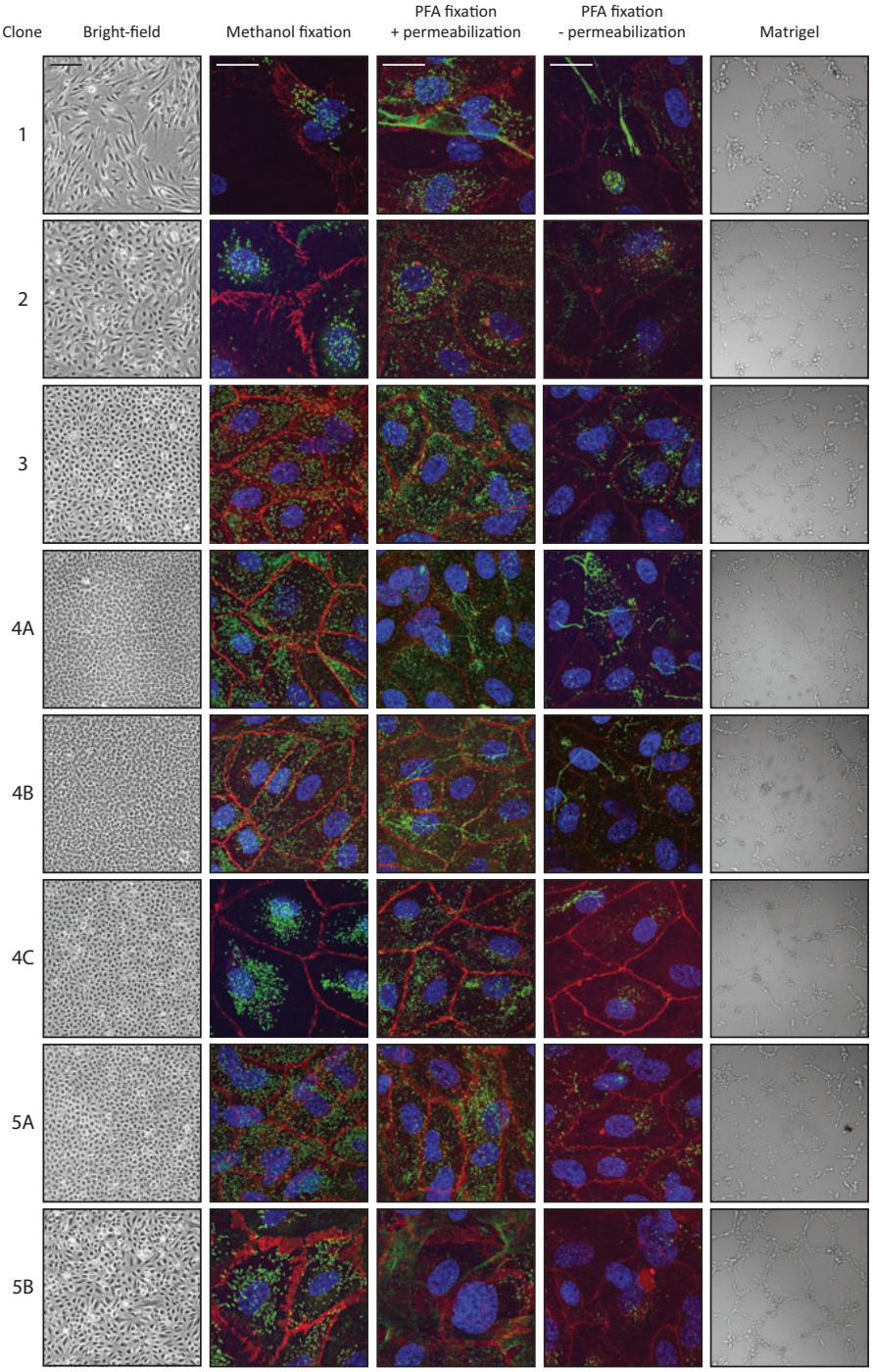
Clone
Bright-field
Methanol fixation
PFA fixation + permeabilization
PFA fixation - permeabilization
Matrigel
1
2
3
4A
4B
4C
5A
5B

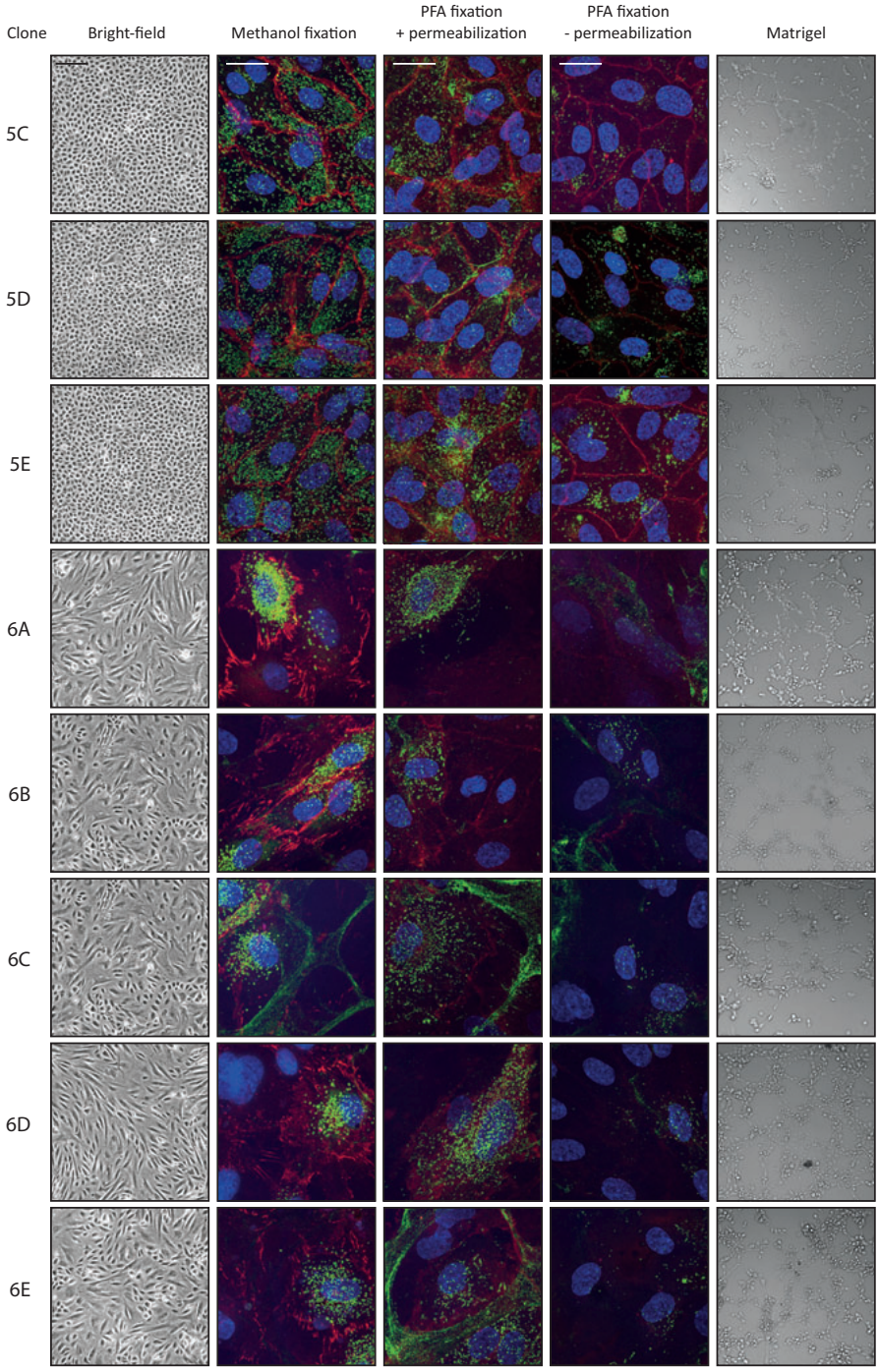

Figure S3. Overview of bright-field, confocal and Matrigel images of all ECFC lines used in this study. First panel: bright-field images of all ECFC lines three to five days after the cells stopped expanding. Bright-

field images show clear morphological variation between ECFC lines. Scale bar in bright-field images represent 200 µm. Second, third and fourth panels: 2x zoom confocal images of all ECFC lines three to five days after the cells stopped expanding, stained for VWF (green) and VE-cadherin (red). Second panel shows intracellular VWF staining after methanol fixation. Third panel shows the intra- and extracellular VWF staining after PFA fixation with permeabilization. Fourth panel shows the extracellular VWF staining after PFA fixation without permeabilization. Scale bar in confocal images represent 10 µm. Images were taken with the Leica TCS SP8 X WLL confocal microscope with a 63x/1.40 NA Plan Apo oil immersion objective. Fifth panel: Matrigel images of all ECFC lines. Images were taken with the Leica AF6000LX with a 10x magnification. ECFC, endothelial colony forming cell; PFA, paraformaldehyde; VWF, von Willebrand factor

Figure S4

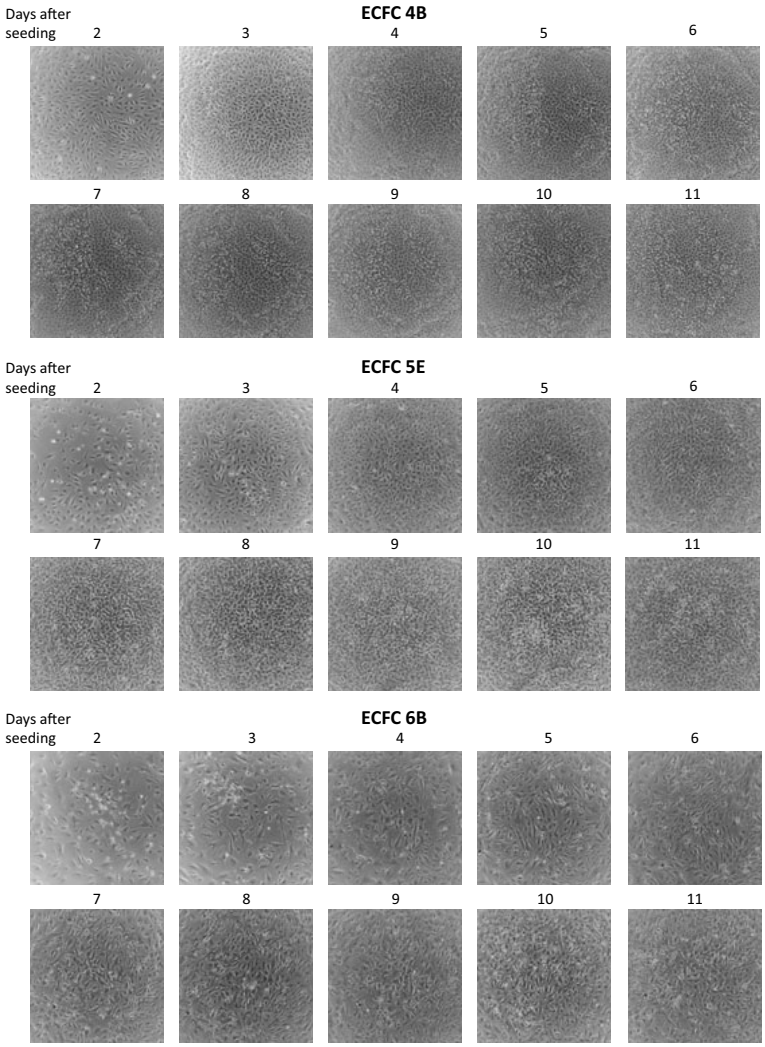

Figure S4. Bright-field images of three representative cell lines followed for eleven days. Bright-field images were taken from cells every day to follow the cell density and determine the optimal time-point to perform experiments. Three representative cell lines are shown, one with a very high (4B), one with an intermediate (5A) and one with a low maximum cell density (6B). ECFC, endothelial colony forming cell

Table S1. qPCR primer list

Primer	Sequence
GAPDH Fw	ACCATCTTCCAGGAGCGAGA
GAPDH Rv	GACTCCACGACGTACTCAGC
VWF Fw	TTGACGGGGAGGTGAATGTG
VWF Rv	ATGTCTGCTTCAGGACCACG
KDR Fw	TGGGAACCGGAACCTCACTATC
KDR Rv	GTCTTTTCCTGGGCACCTTCTATT
ANGPT2 Fw	GGGACAGCCGGCAAAATAAG
ANGPT2 Rv	AAACCACCAGCCTCCTGTTAG
CXCL8 Fw	ACCACCGGAAGGAACCATCT
CXCL8 Rv	AAAACTGCACCTTCACACAGAG
SOX18 Fw	GTGTGGGCAAAGGACGAG
SOX18 Rv	GTTCAGCTCCTTCCACGCT
ACTA1 Fw	ACTGCCTTGGTGTGTGACAA
ACTA1 Rv	CACCATCACCCCCTGATGTC
VIM Fw	GGCGAGGAGAGCAGGATTTC
VIM Rv	TGGGTATCAACCAGAGGGAGT
COL1A1 Fw	CAGCCGCTTCACCTACAGC
COL1A1 Rv	TTTGTATTCAATCACTGTCTTGCC
KLF2 Fw	CACACAGGTGAGAAGCCCTA
KLF2 Rv	ACATGTGCCGTTTCATGTGC
EFNB2 Fw	TGCTGGGGTGTTTTGATGGT
EFNB2 Rv	TCCAGGTAGAAATTTGGAGTTCG
THBD Fw	ACATCCTGGACGACGGTTTC
THBD Rv	CGCAGATGCACTCGAAGGTA

Fw, Forward; Rv, Reverse; ACTA1, α-Smooth Muscle Actin; ANGPT2; angiopoietin-2; COL1A1, collagen Type 1 Alpha 1 Chain; CXCL8, C-X-C Motif Chemokine Ligand 8; EFNB2, Ephrin B2; GAPHD, Glyceraldehyde 3-phosphate dehydrogenase; KDR, Vascular endothelial growth factor receptor 2; KLF2, Krüppel-like Factor 2; SOX18, SRY-Box 18; THBD, Thrombomodulin; VIM, vimentin; VWF, von Willebrand factor